FISEVIER

Contents lists available at ScienceDirect

# Journal of Alloys and Compounds

journal homepage: http://www.elsevier.com/locate/jalcom



# Microstructure, mechanical properties and antibacterial properties of the microwave sintered porous Ti—3Cu alloys



S.C. Tao <sup>a</sup>, J.L. Xu <sup>a, \*</sup>, L. Yuan <sup>b, \*\*</sup>, J.M. Luo <sup>a</sup>, Y.F. Zheng <sup>c, \*\*\*</sup>

- <sup>a</sup> School of Materials Science and Engineering, Nanchang Hangkong University, Nanchang, 330063, PR China
- <sup>b</sup> Institute of Microbiology, Jiangxi Academy of Sciences, Nanchang, 330096, PR China
- <sup>c</sup> Department of Materials Science and Engineering, College of Engineering, Peking University, Beijing, 100871, PR China

#### ARTICLE INFO

Article history:
Received 17 May 2019
Received in revised form
18 July 2019
Accepted 1 September 2019
Available online 3 September 2019

Keywords: Porous Ti—Cu alloy Microwave sintering Mechanical property Antibacterial property Biomedical application

#### ABSTRACT

The porous Ti–3Cu alloys were fabricated by microwave sintering using Mg space holder for biomedical application, and the effects of sintering temperatures on the pore structure, phase composition, compressive strength, elastic modulus, corrosion resistance and antibacterial properties of the porous Ti –3Cu alloys were investigated. The results show that the porous Ti–3Cu alloys are composed of  $\alpha$ -Ti phase and Ti<sub>2</sub>Cu phase, and the intensity of Ti<sub>2</sub>Cu diffraction peaks increases with increasing the sintering temperatures. The sintering temperatures have significant effect on the pore structure of the porous Ti–3Cu alloys, and the porosities decrease with increasing the sintering temperatures. Correspondingly, both of the compressive strength and elastic modulus of the porous Ti–3Cu alloys gradually increase with increasing the sintering temperatures. The elastic modulus of the porous Ti–3Cu alloys is very close to the human cortical bone, while the compressive strength is much higher than that of the human cortical bone. The corrosion resistance of the porous Ti–3Cu alloys in the SBF solution slightly increases with increasing the sintering temperatures. The porous Ti–3Cu alloys exhibit strong antibacterial ability, and the antibacterial rates greatly increase with prolonging the incubation times. After incubation for 12 h, the antibacterial rates of porous Ti–3Cu alloys against both *E. coli* and *S. aureus* are up to 100%.

© 2019 Elsevier B.V. All rights reserved.

#### 1. Introduction

Although titanium and its alloys are receiving increasingly attention in the orthopedic and dental implants field, due to their excellent mechanical properties (high strength and low elastic modulus), good corrosion resistance and excellent biocompatibility [1,2]. However, two major problems have arisen after the actual use of titanium and titanium alloys in the clinic, including bacterial infection [3] and "stress-shielding" effect [4]. The average infection rate of orthopedic metal implants (such as joint prostheses and fracture fixation devices) is as high as 2%–5% shown from current survey results, and the actual infection rate of bacterial infection around the implant may be much higher [5]. Therefore, in order to

E-mail addresses: jlxu@nchu.edu.cn (J.L. Xu), yuanlinjxas@126.com (L. Yuan), yfzheng@pku.edu.cn (Y.F. Zheng).

enhance the antibacterial properties of the implants, antibacterial elements ( $Cu^{2+}$ ,  $Ag^+$  and  $Zn^+$ ) [6–8] have been introduced into the titanium and titanium alloys to develop the antibacterial titanium alloys. Considering the economic cost, antimicrobial efficiency, cytotoxicity and stable reaction of these elements, copper element will be one of the most promising alloy elements in clinical applications [9,10]. Previous studies [11–13] confirmed that the antibacterial rates of the Ti–Cu alloys (Cu content  $\geq$ 5 wt%) against *E. coli* and *S. aureus* are 99.99% after incubation for 24 h. Considering that the excessive copper intake can cause metal toxicity and harm the human body [14], titanium alloy with lower copper content deserves further study.

On the other hand, it is well known that the elastic modulus of titanium and titanium alloys are higher than 100 GPa, much higher than that of natural bone (1–30 GPa) [1,2,15], and the stress is not well transferred from the implant to the adjacent bone tissue (so-called "stress shielding"), causing the growth of the bone tissue around the implant to be blocked, which may cause loosening of the implant and eventual premature failure of the implant [15,16]. Therefore, in order to reduce the elastic modulus, the pore structure

<sup>\*</sup> Corresponding author.

<sup>\*\*</sup> Corresponding author.

<sup>\*\*\*</sup> Corresponding author.

has been introduced into the Ti alloys to form the porous Ti alloys. The porous structure not only reduces the elastic modulus of the implants, but also promotes the ingrowth of new bone cells and tissues, resulting in the tightly fixation between human bones and implants [4,17–19]. Moreover, it can be clearly found from the stress-strain curves in the previous reports that the elastic modulus of the Ti–Cu alloys is much higher that of dense Ti [11,12,20]. Li et al. [21] found that the elastic modulus of the porous Ti–10Cu alloy could decrease to 3–18 GPa using conventional sintering with NH<sub>4</sub>HCO<sub>3</sub> as the space holder agent.

In recent years, conventional sintering with vacuum or atmosphere protection [21,22], self-propagating high-temperature synthesis (SHS) [23], hot isostatic pressing (HIP) [24], spark plasma sintering (SPS) [25,26], 3D printing [27,28] and microwave sintering (MWS) [28–30] have been commonly employed to prepare the porous materials. Among these techniques, microwave sintering is a newly developed rapid sintering method for ceramics, semiconductors, metals and composites [31,32], having been successfully used to prepare the porous metallic alloys for biomedical applications [28–30]. Microwave sintering is a process in which the powder compacts, coupled with microwaves, absorb the electromagnetic energy volumetrically, which transforms into the thermal energy to heat the compacts to sintering temperature, and the densification and alloying are eventually realized [31,32]. Compared with conventional sintering, it has some unique advantages of volumetric heating, reduced sintering time, lowered sintering temperature, enhanced element diffusion process and improved physical and mechanical properties of the sintered materials [31,32]. Therefore, in order to decrease the elastic modulus and Cu content of Ti-Cu alloys, the porous Ti-3Cu alloy was prepared by microwave sintering using Mg powders as the space holder agent in this paper. The effect of the microwave sintering temperatures on the microstructure, mechanical properties, corrosion resistance and antibacterial properties of the porous Ti-3Cu alloys was investigated. At the same time, the effect of incubation times on the antibacterial rates of the porous Ti-3Cu alloy against E. coli and S. aureus was also evaluated detailedly.

# 2. Material and methods

# 2.1. Preparation of the porous Ti-3Cu alloys

Commercially available dehydride titanium powders (purity of  $99.9\,wt\%\text{, average particle size of }10\,\mu\text{m})$  and copper powders (purity of 99.99 wt%, average particle size of 5 μm), with a nominal mass ratio of 97 to 3, were used to prepare the porous Ti-3Cu alloys. The Ti-3Cu mixed powders were blended in a planetary ball mill (QM-3SP4, Nanjing University Instrument Plant, China) at speed of 250 r/min for 6 h. Ball milling was carried out using steel balls with a constant ball to powder ratio of 3:1 at room temperature. Then, 5 wt% Mg powders (purity of 99.99 wt%, average particle size of 75 μm) were thoroughly mixed into the Ti–3Cu powders as the space holder agent for 3 h. The mixed Ti-3Cu-5Mg powders were cold-pressed into green compacts ( $\Phi$ 12 mm  $\times$  8 mm) under a uniaxial pressure of 580 MPa for 1 min. Afterwards, the green compacts were put into an alumina crucible with SiC particles as the microwave acceptor, and simultaneously the alumina crucible was put inside a mullite fiber cotton insulation barrel. At last, the insulation barrel was put into a 2.45 GHz 5 kW microwave sintering furnace (NJZ4-3, Nanjing Jiequan co., Ltd., China). The green compact samples were sintered by microwave heating at a rate of 10 °C/min to 650, 700, 750 and 800 °C for 20 min, respectively, and cooled in furnace down to room temperature. During sintering process, an infrared pyrometer was used to monitor the temperature of the sintered samples and the microwave sintering furnace was filled with flowing high purity argon gas (purity>99.999%) to prevent the oxidation of the sintered samples. At the same time, the porous Ti samples used as the control were prepared using titanium powders and 5 wt% Mg powders with the same sintering process at  $800\,^{\circ}\text{C}$ .

#### 2.2. Microstructural characterization

The sintered porous Ti-3Cu alloys were successively ground with SiC sandpaper down to 2000 grits, and then polished with Cr<sub>2</sub>O<sub>3</sub>, followed by ultrasonically cleaned in acetone and distilled water, respectively. The porous structure of the polished porous Ti-3Cu alloys was inspected by an optical microscopy (DM1500, Shenzhen Hipower Optoelectronics Co., Ltd., China). The polished and fractured surface morphologies of the sintered Ti-3Cu alloys were investigated by a scanning electron microscopy (SEM, SU1510 HITACHI, Japan) equipped with energy dispersive X-ray (EDS, Oxford Instruments INCA 6650, England). The phase constituents of porous Ti-Cu alloys were identified by X-ray diffraction (XRD, Bruker D8 FOCUS, Germany). The actual porosity (*P*) of the porous Ti-3Cu alloys was investigated by Archimedes law according to ASTM B962-08 and the theoretical density of Ti-3Cu alloy was calculated based on the measured value of 4.61 g/cm<sup>3</sup> [29], in which the densities of pure titanium and copper were 4.51 g/cm<sup>3</sup> and 8.92 g/cm<sup>3</sup>, respectively.

### 2.3. Compressive test

Uniaxial compression tests were conducted on cylindrical porous Ti—3Cu alloys with a length of 3 mm and diameter of 6 mm (L/D=2.0, ASTM E9-09). The compressive tests were carried out under room temperature with a cross-head velocity of 0.2 mm/min on an electronic universal testing machine (WDW-50, Jinan Shijin group Co., Ltd., China). For the compressive test, at last three samples were tested for each group, and the results were calculated as average values  $\pm$  standard deviation.

## 2.4. Electrochemical test

The corrosion resistance of the porous Ti—3Cu samples in the SBF solution (NaCl 8.03 g/L, KCl 0.22 g/L, Na<sub>2</sub>SO<sub>4</sub> 0.07 g/L, NaHCO<sub>3</sub> 0.35 g/L, K<sub>2</sub>HPO<sub>4</sub>·3H<sub>2</sub>O 0.23 g/L, MgCl<sub>2</sub>·6H<sub>2</sub>O 0.31 g/L, CaCl<sub>2</sub> 0.28 g/L) at room temperature was evaluated by potentiodynamic polarization test through an electrochemical analyzer (CHI650D, Shanghai Chenhua instrument Co. Ltd., China). The electrochemical test was conducted using a conventional three electrodes electrochemical cell with a saturated calomel electrode (SCE) as the reference, the samples with the area of 1 cm<sup>2</sup> as the working electrode, and a Pt foil as the auxiliary electrode. The polarization scan ranged from OCP-0.6 V-1.5 V with the scan rate of 0.5 mV/s.

# 2.5. Antibacterial test

All of the samples for antibacterial test were cut into  $\Phi10\,\text{mm}\times2\,\text{mm},$  ground with SiC paper up to 2000 grits and polished with  $\text{Cr}_2\text{O}_3.$  Nutrient broth (NB) was selected as the solid medium, which was dissolving 10.0 g peptone, 5.0 g beef extract, 5.0 g NaCl and 15.0 g agar in 1000 mL distilled water and the pH value was adjusted to 7.2 to 7.4. Nutrient broth (NB) without agar was selected as the liquid medium and the pH value was adjusted to 7.2 to 7.4. Saline solution (0.9% NaCl solution) was selected as the dilution solution. All of the samples, solid medium, liquid medium and saline solution were sterilized by autoclaving at 121 °C for 20 min. For examining bacterial proliferation, the samples were exposed to gram positive S. aureus, strain ATCC 25923 and gram

negative *E. coli*, strain MG1455. The *S. aureus* and *E. coli* were cultivated at  $37\,^{\circ}$ C in the liquid medium to a concentration of  $10^9\,\text{cfu/mL}$  in 12 h, and then were diluted 100-fold by saline solution to a concentration of  $10^7\,\text{cfu/mL}$  (bacterial suspension).

Plate counting method was conducted with reference to the National Standard of China GB/T 2591 (equivalent to JIS Z 2801-2000, ASTM G21-96, NEQ) [33].  $5\,\mu\text{L}$  of the bacterial suspension were inoculated on the samples, and then the samples were covered by glass in a sterile dish and incubated at 37 °C for 3, 6, 12 and 24 h. Each sample was washed using 5 mL saline solution.  $50\,\mu\text{L}$  of the bacterial culture solution was spread onto the Petri dish containing solid medium. After 24 h, the number of colonies was counted. The antibacterial rate (R) could be calculated by the following formula [11–13]:

$$R = (N_{\text{control}} - N_{\text{sample}}) / N_{\text{control}} \times 100\%$$
 (1)

where  $N_{\rm control}$  and  $N_{\rm sample}$  are the numbers of the bacterial colony on the control sample (the porous Ti) and the porous Ti–3Cu alloys, respectively. Three samples were tested for each group in anti-bacterial experiments.

### 3. Results and discussion

3.1. Microstructure and phase composition of the porous Ti-3Cu alloys

The polished surface optical micrographs of the porous Ti–3Cu alloys prepared by microwave sintering at different temperatures are shown in Fig. 1. There are many large pores (~120  $\mu$ m) and small pores (~15  $\mu$ m) randomly distributed over the surface of the porous

Ti-3Cu alloys, and the average size of large pores decreases from 130 μm for 650 °C to 100 μm for 800 °C with increasing the sintering temperatures. At the same time, the number of small pores on the surface of porous Ti-3Cu alloys decreases gradually with increasing the sintering temperatures. The large pores should be mainly derived from the evaporation of Mg space holder agents. and the shapes of the pores are also inherited from the shapes of Mg powders. The small pores can be attributed to the gap between the powders (interparticle pores), the evaporation of impurities in the green compact and Kirkendall pores [34,35]. With increasing the sintering temperature, the volume shrinkage of the sintered samples increases, especially for 800 °C, which leads to the corresponding decrease of the large pores size. Meanwhile, some small pores may be merged into the large ones or disappear due to the closure of the sintering necks, resulting in a great decrease in the number of small pores.

Fig. 2 shows the polished surface and fractured surface SEM images of the porous Ti—3Cu alloys prepared at 650 °C and 800 °C. It can be seen that there are also many large pores and small pores distributed over the porous Ti—3Cu alloys, and the size of large pores slightly decreases and the number of small pores greatly decreases as increasing the sintering temperature to 800 °C. The SEM morphological evolution regularity of the porous Ti—3Cu alloy prepared at different sintering temperatures is strongly consistent with the optical micrographs. Moreover, the interparticle pores are obviously observed in the porous Ti—3Cu alloy prepared at 650 °C (seen in inset of Fig. 2a and c) due to the incompletely sintering, while the interparticle pores greatly decrease as the sintering temperature increases to 800 °C (seen in inset of Fig. 2b and d) due to the formation and growth of sintered necks, indicating that the alloying and densification processes are more complete as the

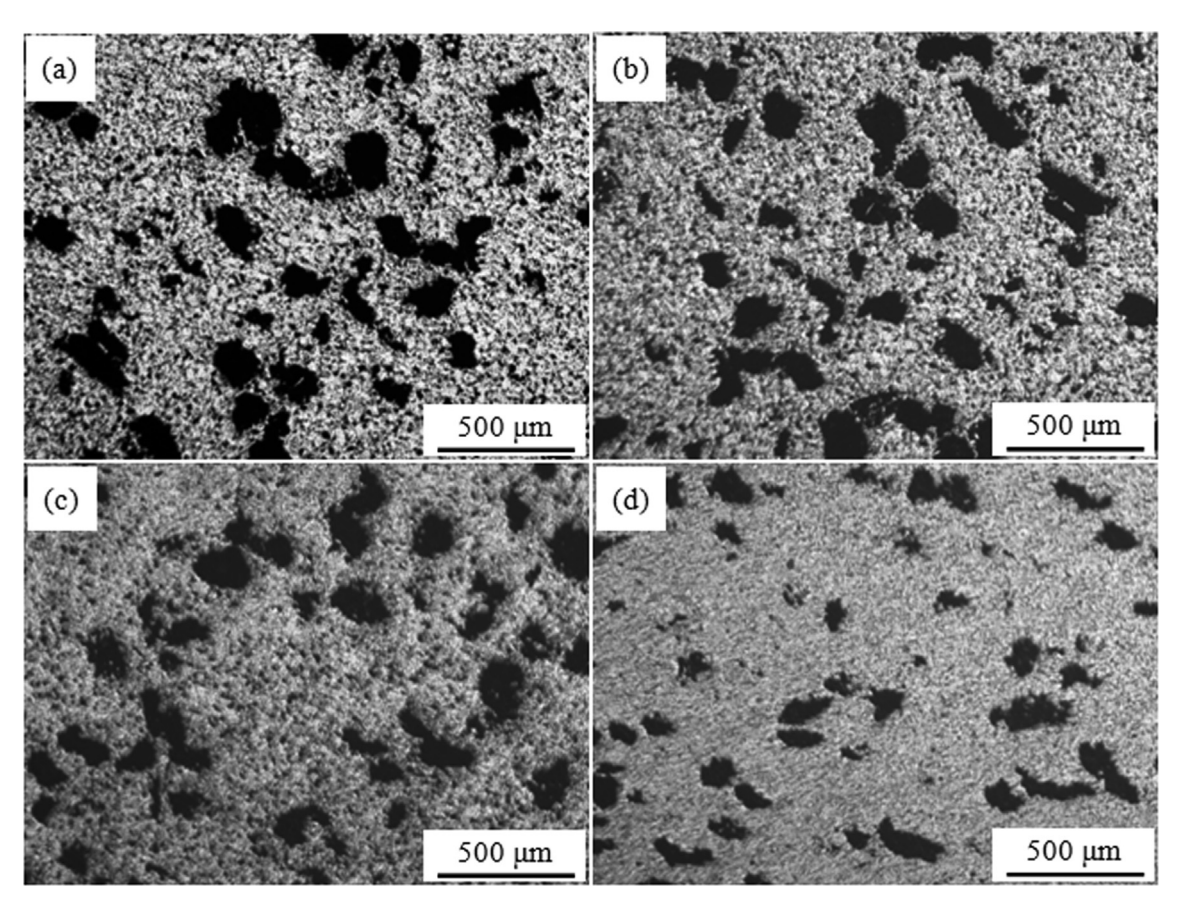


Fig. 1. The polished surface optical micrographs of the porous Ti-3Cu alloys prepared at different temperatures: (a) 650 °C; (b) 700 °C; (c) 750 °C; (d) 800 °C.

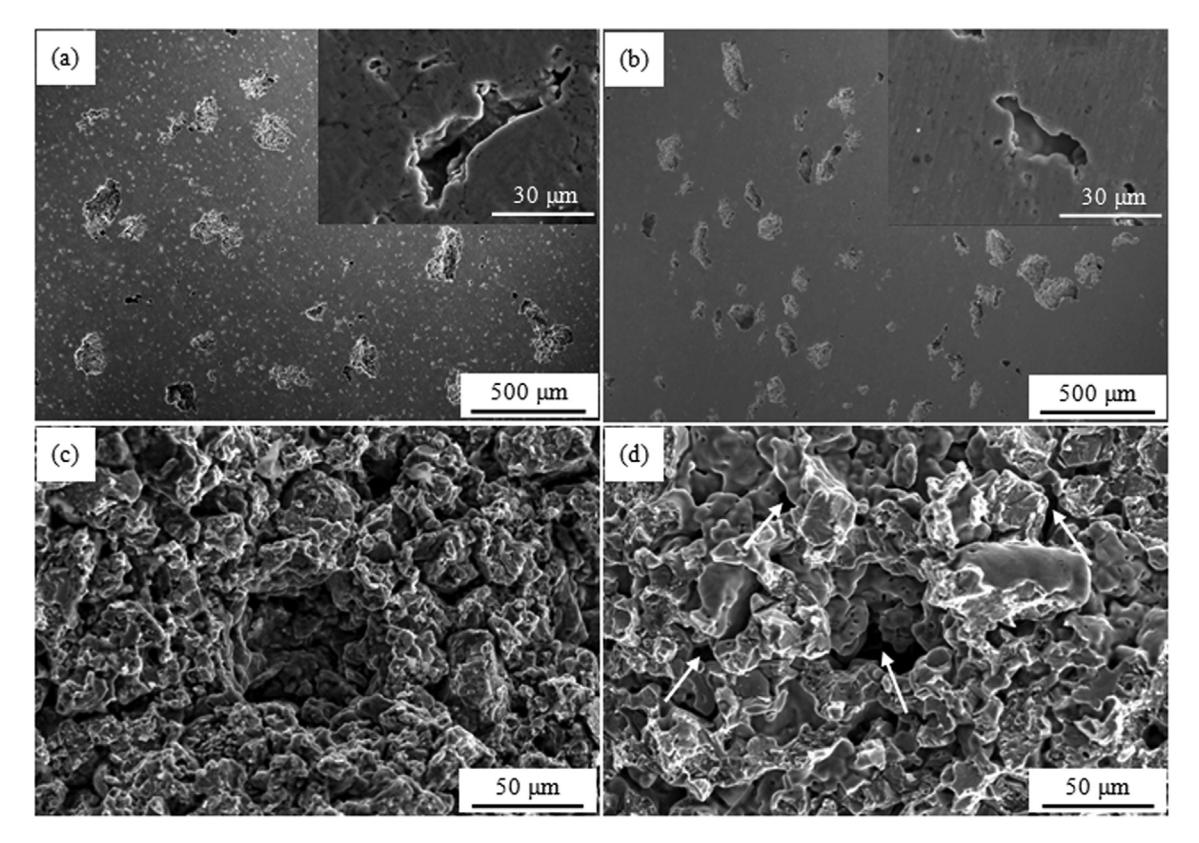


Fig. 2. The polished surface (a) (b) and fractured surface (c) (d) SEM images of the porous Ti-3Cu alloys prepared at different temperatures: (a) and (c) 650 °C; (b) and (d) 800 °C (White arrows mark the interconnected pores).

sintering temperature increases to  $800\,^{\circ}$ C. Moreover, some interconnected pores also can be observed from Fig. 2d (indicated by white arrows), which illustrates that the porous structure of the Ti–3Cu alloys should be three-dimensional connectivity.

The porosities and densities of the porous Ti-3Cu alloys prepared by microwave sintering at different temperatures are shown in Fig. 3. The densities of the porous Ti-3Cu alloys increase with increasing the sintering temperatures, while the porosities decrease accordingly. The density of the porous Ti-3Cu sample with a sintering temperature of  $650\,^{\circ}C$  is about  $3.35\,g/cm^3$ , and it increases to  $3.64\,g/cm^3$  for sintering temperature of  $800\,^{\circ}C$ . While

the porosity decreases from 27.25% for sintering temperature of  $650\,^{\circ}\text{C}$  to 21.08% for sintering temperature of  $800\,^{\circ}\text{C}$ . The results of porosities are strongly consistent with the microstructure evolution of porous Ti–3Cu alloys.

The XRD patterns of the porous Ti-3Cu alloys prepared by microwave sintering at different temperatures are shown in Fig. 4, the Ti-3Cu-5Mg compact as the control. Except the diffraction peaks of  $\alpha$ -Ti, Cu and Mg, without any other peaks are detected in the Ti-3Cu-5Mg compact, indicating that no reaction happens and

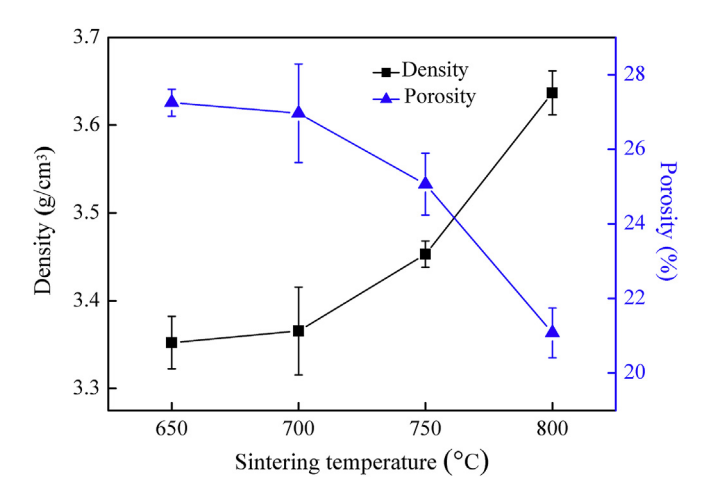


**Fig. 3.** Relationship between sintering temperatures and porosities and densities of the porous Ti–3Cu alloys.

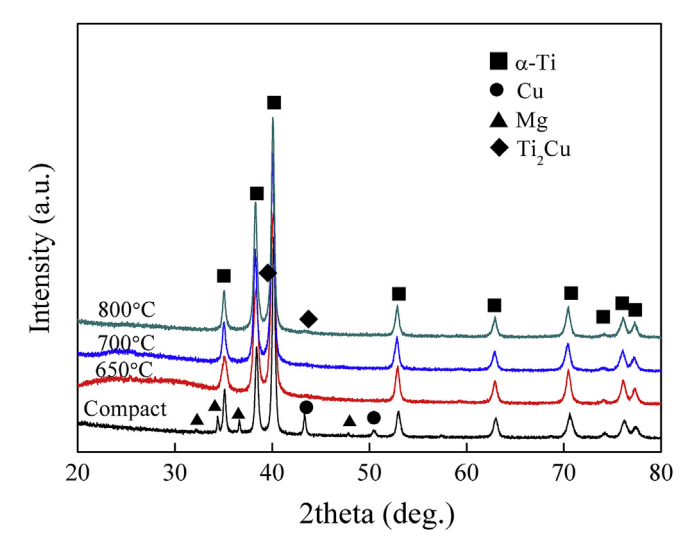


**Fig. 4.** XRD patterns of the Ti-3Cu-5Mg compact and the porous Ti-3Cu alloys prepared at different temperatures.

any impurities incorporated along titanium powder, copper powder and magnesium powder during the ball milling. After sintering at 650 °C, 700 °C and 800 °C, dominant  $\alpha$ -Ti phases are clearly detected, while the peaks of magnesium are not detected, indicating that magnesium as the space holder agent, has almost completely evaporated at the sintering temperature from 650 °C to 800 °C. The diffraction peaks of copper phase were also not observed, while the diffraction intensities of Ti<sub>2</sub>Cu phase increase with increasing the sintering temperatures, indicating that the contents of Ti<sub>2</sub>Cu increase correspondingly. This result is similar to the result of Yao's report [36]. When the sintering temperature is up to 800 °C, two diffraction peaks can be clearly observed at 39.5° and 43°, corresponding to the Ti<sub>2</sub>Cu phase.

In order to further confirm the existence of the  $Ti_2Cu$  phase, the SEM image and EDS analyses of the porous Ti-3Cu alloy prepared at  $800\,^{\circ}C$  are shown in Fig. 5. It can be observed from Fig. 5a that the off-white strip or lump substances are randomly distributed over surface of porous Ti-3Cu alloy. According to the EDS map scanning results, the off-white substances are mainly composed of Ti and Cu elements, and the atomic ratio of Ti and Cu (B point) is very close to 2:1 (seen in Fig. 5d), indicated that the off-white substances are corresponding to the  $Ti_2Cu$  phase. On the other hand, the remaining gray location (like A point) is only composed of Ti element, corresponding to the Ti matrix. Therefore, the  $Ti_2Cu$  phases are randomly dispersed over the Ti matrix in various shapes.

### 3.2. Mechanical properties of the porous Ti-3Cu alloys

The typical compressive stress-strain curves of the porous Ti–3Cu alloys prepared at different temperatures are shown in

Fig. 6, and the compressive strength and elastic modulus extracted from the curves are shown in Fig. 7. It can be seen that all of the stress-strain curves contain the elastic deformation process, long plastic deformation process and rupture process, and both of the maximum strain and the maximum stress increase with increasing the sintering temperatures. It can seen from Fig. 7 that both the compressive strength and elastic modulus of the porous Ti—3Cu alloys gradually increase with increasing the sintering temperatures, and the compressive strength increases from 488.51 MPa for

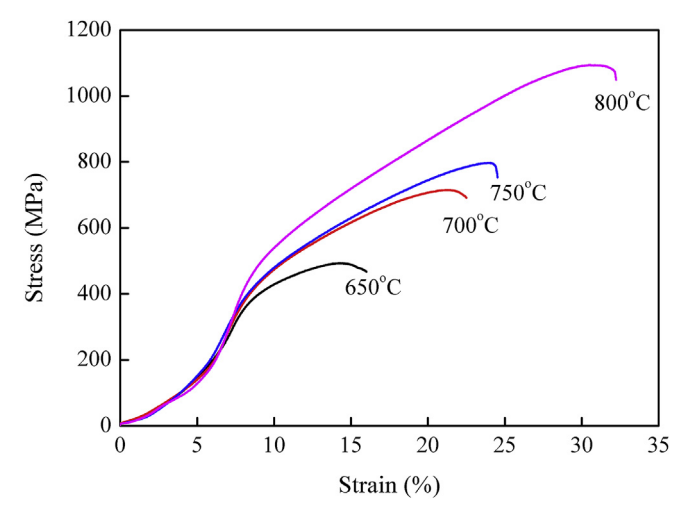


Fig. 6. Compressive stress-strain curves of the porous NiTi alloys prepared at different sintering temperatures.

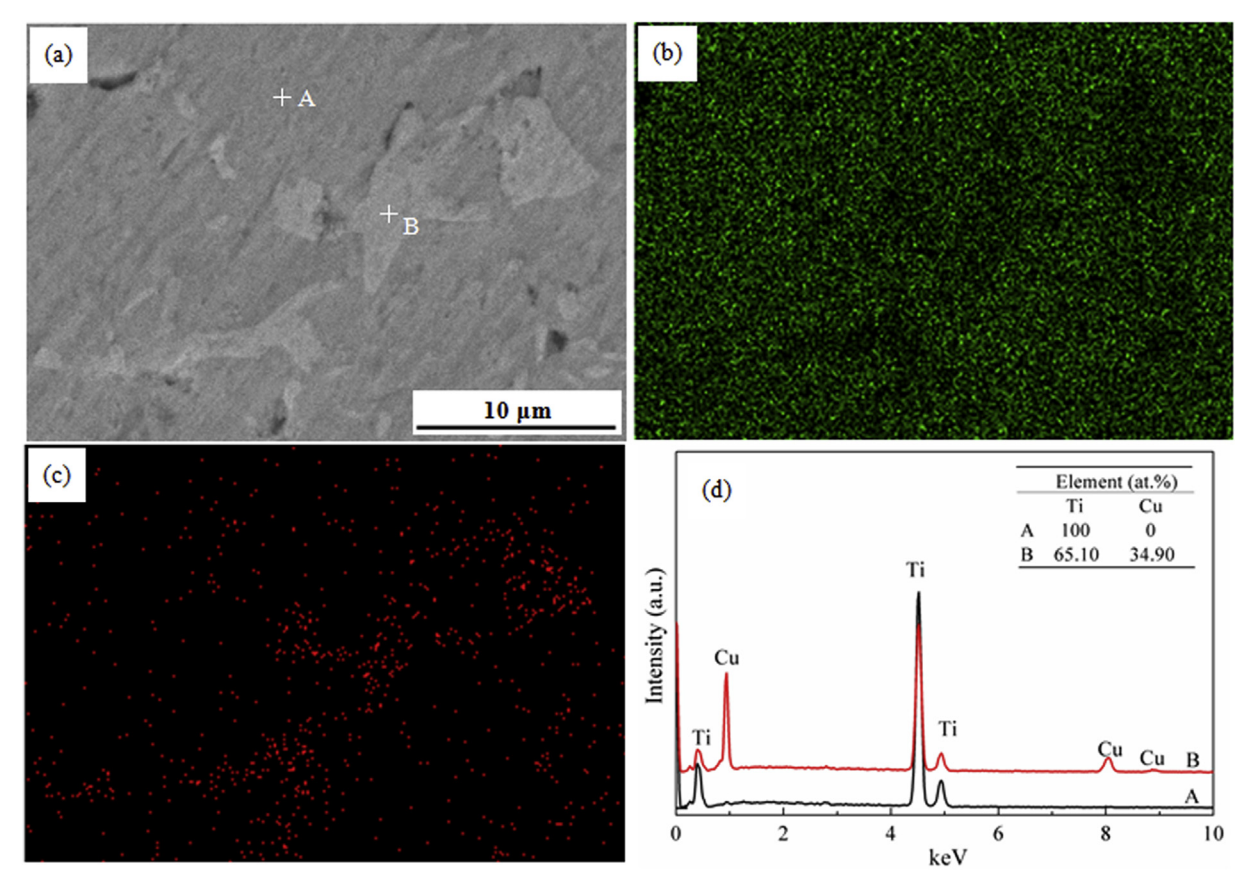


Fig. 5. The SEM image (a), EDS map scanning images of Ti (b) and Cu (c) and EDS point scanning patterns (d) of the porous Ti-3Cu alloy prepared at 800 °C.

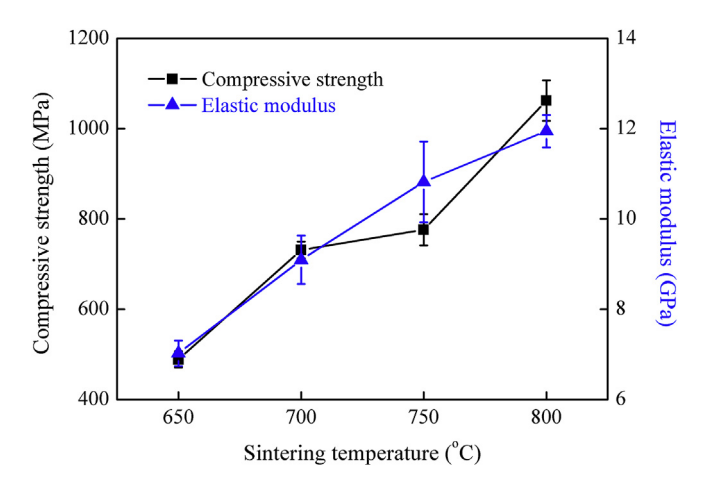


Fig. 7. Compressive strength and elastic modulus of the porous Ti—3Cu alloys prepared at different sintering temperatures.

the porous Ti-3Cu alloy sintered at 650 °C to 1062.34 MPa for 800 °C. Correspondingly the elastic modulus increases from 7.02 GPa for 650 °C to 11.94 GPa for 800 °C. The increase of the porous Ti-3Cu alloys in compressive strength is mainly attributed to the decrease of the porosities and the increase of Ti<sub>2</sub>Cu contents. The elastic modulus of porous Ti-3Cu alloys ranged from 7 to 12 GPa is very close to that of human cortical bone (3–20 GPa) [37]. The compressive strength of the porous Ti-3Cu alloys ranged from 488.51 MPa to 1062.34 MPa is much higher than that of the natural cortical bone (100-230 MPa) [37]. The porous Ti-10Cu alloys were prepared by Li et al. [21] using the conventional sintering with NH<sub>4</sub>HCO<sub>3</sub> as space holder agent, and the compressive strength of the porous Ti-10Cu alloy with the porosity of 24.6% was only 407 MPa, much lower than that of the porous Ti-3Cu allovs with the same porosity (776 MPa). On the other hand, the porous Ti-3Cu with the porosity of 25% was prepared at 750 °C for 20 min, while the porous Ti-10Cu alloy was prepared at 950 °C for 4 h. Therefore, compared to the conventional sintering, the preparation of porous Ti-Cu alloy by microwave sintering with Mg space holder has many advantages, such as low sintering temperature, short holding time and high mechanical properties of sintered samples. Moreover, the strength to modulus ratio is frequently used to evaluate the performance of biomaterials with low elastic modulus and high strength. The higher this ratio is, the more desirable the material for such applications [38,39]. The strength to modulus ratio of the porous Ti-3Cu alloys can be up to  $88.94 \times 10^{-3}$ , much higher than those of other porous Ti alloys [21,29,38–41] or dense Ti alloys [42]. Hence, in terms of the requirements of compressive mechanical behavior, the porous Ti-3Cu alloy fabricated by microwave sintering could be a promising candidate for the hard tissue repair and replacement implant.

### 3.3. Corrosion resistance of the porous Ti-3Cu alloys

Fig. 8 shows the potentiodynamic polarization curves of the porous Ti–3Cu alloys prepared at different temperatures. The corrosion potential ( $E_{corr}$ ), the corrosion current density ( $I_{corr}$ ) and anodic and cathodic Tafel slopes ( $\beta_a$  and  $\beta_c$ ) extracted from the polarization curves using the Tafel extrapolation method are listed in Table 1. The polarization resistance ( $R_p$ ), which represents the corrosion properties of specimens, was calculated using Eq. (2) [43,44]:

$$R_{P} = \frac{\beta_{\alpha} \cdot |\beta_{c}|}{(2.303I_{corr}(\beta_{\alpha} + |\beta_{c}|))}$$
 (2)

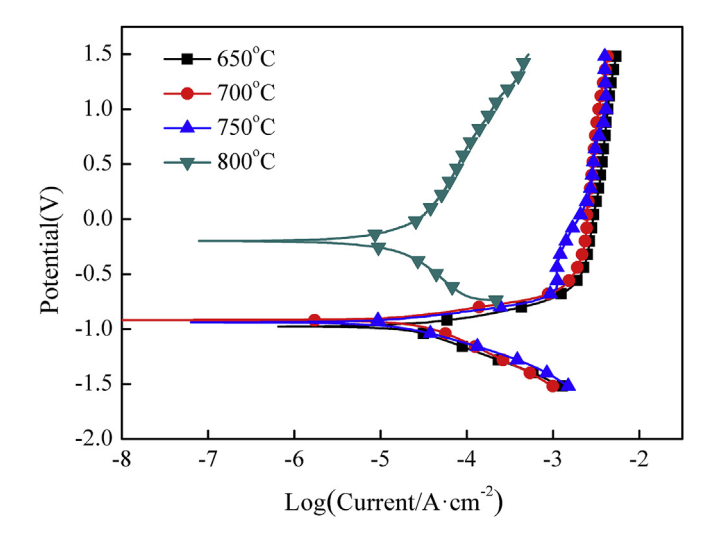


Fig. 8. Potentiodynamic polarization curves of the porous Ti—3Cu alloys prepared at different temperatures.

**Table 1**Corrosion parameters of the porous Ti—3Cu alloys prepared at different temperatures in SBF solution.

Sample	$E_{corr}\left(V\right)$	$I_{corr}$ (A/cm <sup>2</sup> )	$\beta_a$ (V/dec)	$\beta_c$ (V/dec)	$R_p (\Omega/\text{cm}^2)$
650	-0.976	$2.488 \times 10^{-5}$	0.119	0.250	1407
700	-0.917	$1.318 \times 10^{-5}$	0.120	0.224	2040
750	-0.938	$1.039 \times 10^{-5}$	0.097	0.172	2598
800	-0.199	$5.985 \times 10^{-6}$	0.208	0.212	7626

When the sintering temperatures are lower than 800 °C, the potentiodynamic polarization curves of the porous Ti-3Cu alloys almost coincide, indicating that the sintering temperatures have no obvious effect on corrosion resistance of the porous Ti-3Cu alloys. When the sintering temperature is up to 800 °C, a shift of the whole polarization curve towards the region of lower current density and higher potential can be clearly observed, indicating that the porous Ti-3Cu alloy has a significant improvement in the corrosion resistance. It can be seen from Table 1 that the corrosion current density of the porous Ti-3Cu alloys slightly decreases and the polarization resistance increases with increasing the sintering temperatures, which indicates that the corrosion resistance of the porous Ti-3Cu alloys increases with increasing the sintering temperatures. The corrosion current density of the porous Ti-3Cu alloys is equivalent to that of porous Ti-10Cu alloy [21], but it is one or two orders of magnitude higher than those of dense Ti-Cu alloys [11–13]. The decrease in the corrosion resistance of the porous Ti–Cu alloys is mainly attributed to the porous structure with the larger real contact surface area of the porous Ti-Cu alloys than that of the dense Ti-Cu alloys and the probable occurrence of crevice corrosion in the porous structure [45,46]. However, the porous structure and reduced corrosion resistance of the porous Ti-3Cu alloy may be beneficial to the release of Cu ions and improve the antibacterial properties of the alloy. Moreover, no pitting corrosion appearance can be detected from the polarization curves, indicating that the passive film formed on the porous Ti-3Cu alloys surface is not broken even the potentials up to 1.5 V (vs SCE) and suggesting that the porous Ti-3Cu alloys show high corrosion resistance in SBF solution.

# 3.4. Antibacterial ability of the porous Ti-3Cu alloys

The typical E. coli bacterial colonies and S. aureus bacterial

colonies incubated for 24 h on surface of the porous Ti (the control sample) and the porous Ti—3Cu alloys prepared at different sintering temperatures are shown in Fig. 9. Large amounts of *E. coli* bacterial colonies and *S. aureus* bacterial colonies are distinctly observed on the control sample, while no *E. coli* bacterial colony and *S. aureus* bacterial colony can be found on all of the porous Ti—3Cu alloys, indicating that all the antibacterial rates of the porous Ti—3Cu alloys prepared at sintering temperatures from 650 °C to 800 °C against *E. coli* and *S. aureus* are up to 100% after 24 h incubation. It can be proved that the porous Ti—3Cu alloy can be imparted with excellent antibacterial properties when the addition amount of copper is 3 wt%, and the sintering temperatures have no obvious effect on the antibacterial properties of the porous Ti—3Cu alloys.

The typical bacterial colonies incubated from *E. coli* and *S. aureus* suspensions are shown in Fig. 10, which have been incubated with the porous Ti—3Cu alloy prepared at 800 °C for 3 h, 6 h and 12 h, respectively. Large amounts of *E. coli* bacterial colonies and *S. aureus* bacterial colonies are observed on the control sample when the incubation time from 3 h to 12 h (not shown), confirming that the porous Ti does not have the antibacterial ability. When the *E. coli* bacterial and *S. aureus* bacterial are incubated on the porous Ti—3Cu alloys for 3 h, only a few bacteria are survived. While the *E. coli* and *S. aureus* suspensions are incubated with the porous Ti—3Cu alloy for 6 h, only a few *S. aureus* bacterial colonies can be observed, and no *E. coli* bacterial colonies are survived. Further prolonging the incubation time to 12 h, no *E. coli* bacterial colony and *S. aureus* 

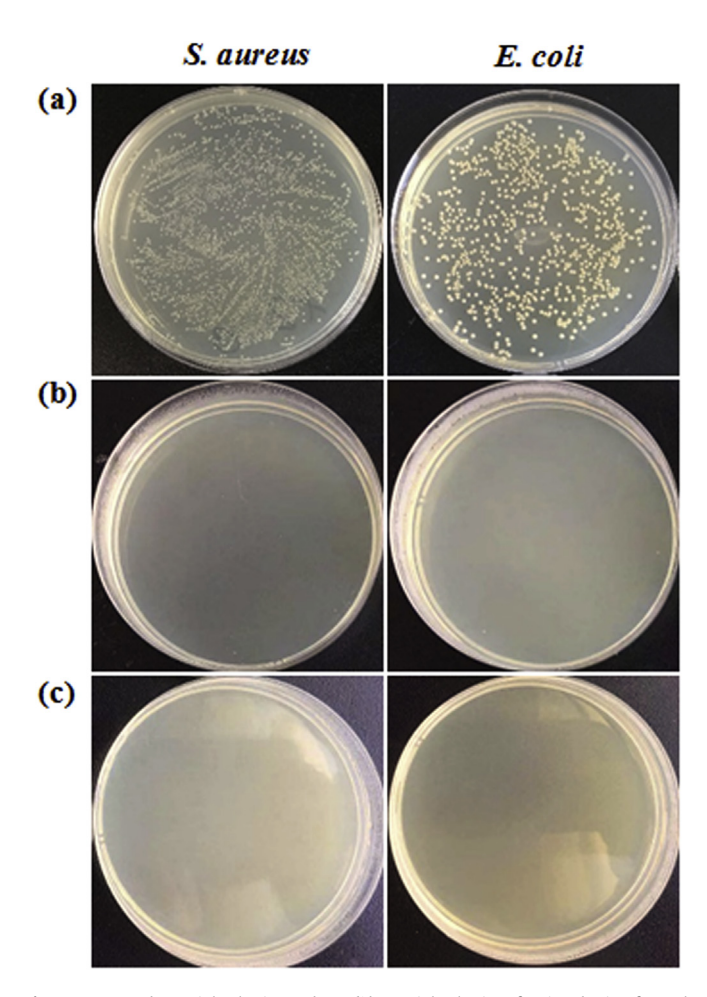


**Fig. 9.** *S. aureus* bacterial colonies and *E. coli* bacterial colonies after incubation for 24 h on the control sample (a) and the porous Ti-3Cu alloys prepared at  $650 \,^{\circ}C$  (b) and  $800 \,^{\circ}C$  (c).

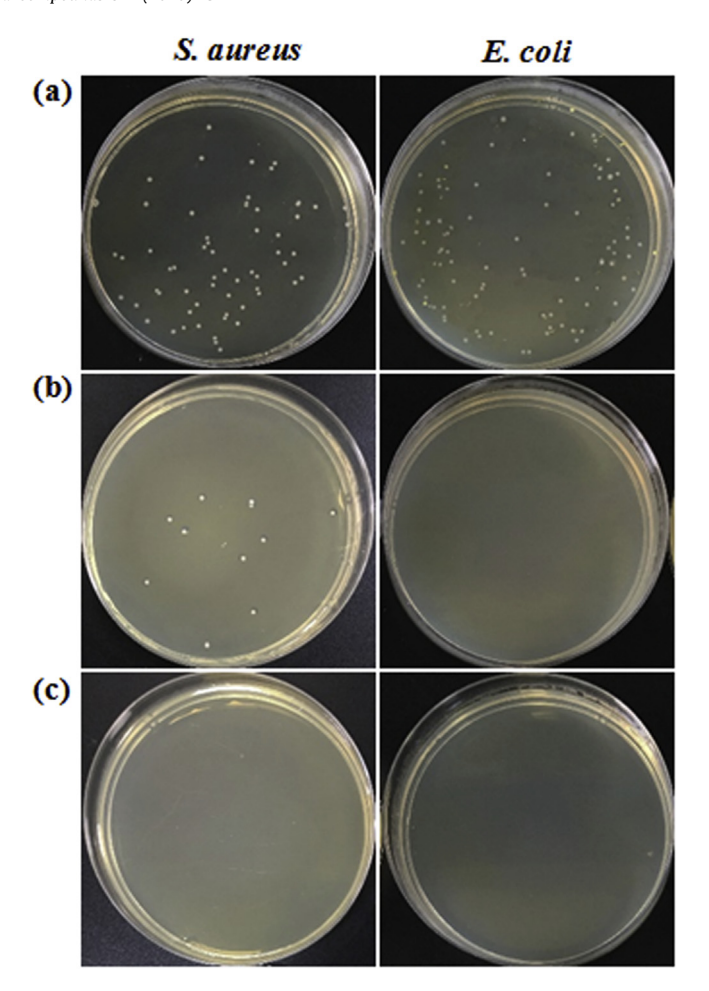


**Fig. 10.** *S. aureus* bacterial colonies and *E. coli* bacterial colonies after incubation for different times on the porous Ti-3Cu alloys prepared at  $800\,^{\circ}C$ : (a)  $3\,h$ ; (b)  $6\,h$ ; (c)  $12\,h$ .

bacterial colony can be found on the porous Ti-3Cu alloy.

The antibacterial rate-incubation time curves of the porous Ti—3Cu alloy prepared at 800 °C are shown in Fig. 11. The antibacterial rates of the porous Ti—3Cu alloy greatly increase with increasing the incubation times, and then keep steady at 100% after incubation for 12 h. The antibacterial rates of porous Ti—3Cu alloy against *E. coli* and *S. aureus* for 3 h are 81.3% and 88.2%, respectively. The antibacterial rates of porous Ti—3Cu alloy against *S. aureus* for 6 h reaches 98.1%, while the antibacterial rates against *E. coli* is almost 100%. When the incubation time is prolonged to 12 h, the antibacterial rates of porous Ti—3Cu alloy against both *E. coli* and *S. aureus* are up to 100%.

The antibacterial properties of porous Ti—3Cu alloys in this study are significantly better than those of the previous reports [12,47–50], such as lower copper content (3 wt%) and shorter sterilization time (6–12 h). Liu et al. [12] reported that the content of Cu in Ti—Cu alloys should be higher than 5 wt% to obtain high and stable antibacterial performance against *S. aureus* and *E. coli*. The antibacterial rates of the smelted Ti—5Cu alloy against *E. coli* and *S. aureus* for 12 h are just 96% and 80% [47].The antibacterial rate of the wrought Ti—3Cu alloy to *S. aureus* for 36 h is only 99.32% [48]. Liu et al. [49] found that the antibacterial rates of the Ti—10Cu samples against *E. coli* and *S. aureus* were 36% and 43% for 3 h incubation, respectively. Fowler et al. [50] also reported that Ti—3Cu alloys showed antibacterial property with an antibacterial rate of 16% for 6 h incubation. The structure and phase composition of the

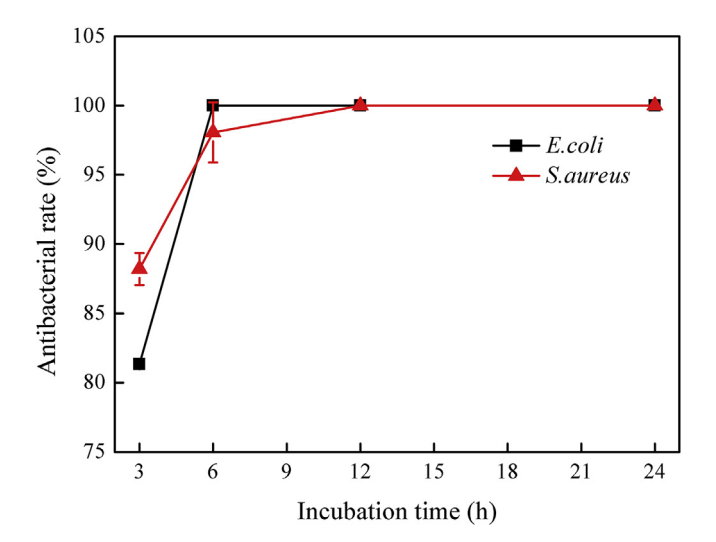


**Fig. 11.** Antibacterial rate-incubation time curves of the porous Ti-3Cu alloy prepared at  $800\,^{\circ}C$ .

microwave sintered porous Ti-3Cu alloy may be ascribed for its excellent antibacterial properties. First, the porous structure of the porous Ti-Cu alloy greatly increases the contact area between the alloy and bacteria [51]. Second, the porous structure increases the superficial area and reduces the corrosion resistance of the Ti-Cu alloy, which is beneficial to the release of Cu<sup>2+</sup> ions and improvement of the antibacterial ability. Third, the porous structure may cause piercing, deformation, and damage of the cellular membranes, which leads to bacterial cell death and plays an important role in antibacterial ability [52]. Finally, the fine Ti<sub>2</sub>Cu phase is formed during the sintering process, which can make sure that the porous Ti-3Cu alloy has excellent antibacterial properties [13]. Actually, the detailed antibacterial mechanism of the porous Ti-3Cu alloys need to be further explored in the future. Therefore, only considering the mechanical and antibacterial properties, the porous Ti-3Cu alloy with low modulus, high strength and strong antibacterial ability will be a very promising alternative material for hard tissue repair and replacement.

## 4. Conclusions

- (1) The porous Ti–3Cu alloys were successfully prepared by microwave sintering using Mg space holder. The porous Ti–3Cu alloys consisted of  $\alpha$ -Ti and Ti<sub>2</sub>Cu phases, and the diffraction peaks of Ti<sub>2</sub>Cu phase increased with increasing the sintering temperatures.
- (2) The size of large pores increased and the number of small pores decreased with increasing the sintering temperatures, while the porosities of the porous Ti—3Cu alloys decreased, which leaded to the corrosion resistance slightly enhanced.
- (3) The compressive strength and elastic modulus of the porous Ti—3Cu alloys gradually increased with increasing the sintering temperatures, and the elastic modulus was very close to that of the natural cortical bone.
- (4) The antibacterial rates of the porous Ti—3Cu alloys greatly increased with prolonging the incubation times. After incubation for 12 h, the antibacterial rates of porous Ti—3Cu alloys against both *E. coli* and *S. aureus* were up to 100%.

# Acknowledgements

The authors gratefully acknowledge the financial support of the

project from the National Natural Science Foundation of China (51101085, 51764041), the Natural Science Foundation of Jiangxi Province (2016BAB206109).

#### References

- [1] Q. Chen, G.A. Thouas, Metallic implant biomaterials, Mater. Sci. Eng. R 87 (2015) 1–57.
- [2] M. Geetha, A.K. Singh, R. Asokamani, A.K. Gogia, Ti based biomaterials, the ultimate choice for orthopaedic implants-A review, Prog. Mater. Sci. 54 (2009) 397–425.
- [3] H.J. Busscher, H.C. van der Mei, G. Subbiahdoss, P.C. Jutte, J.J. van den Dungen, S.A. Zaat, M.J. Schultz, D.W. Grainger, Biomaterial-associated infection: locating the finish line in the race for the surface, Sci. Transl. Med. 4 (2012) 2569–2575.
- [4] G. Lewis, Properties of open-cell porous metals and alloys for orthopaedic applications, J. Mater. Sci. Mater. Med. 24 (2013) 2293–2325.
- [5] M. Deysine, Infections associated with surgical implants, N. Engl. J. Med. 351 (2004) 193–195.
- [6] X. Wang, H. Dong, J. Liu, G. Qin, D. Chen, E. Zhang, In vivo antibacterial property of Ti-Cu sintered alloy implant, Mater. Sci. Eng. C 100 (2019) 38–47.
- [7] B. Szaraniec, T. Goryczka, Structure and properties of Ti-Ag alloys produced by powder metallurgy, J. Alloy. Comp. 709 (2017) 464–472.
- [8] L. Zhang, J. Guo, T. Yan, Y. Han, Fibroblast responses and antibacterial activity of Cu and Zn co-doped TiO<sub>2</sub> for percutaneous implants, Appl. Surf. Sci. 434 (2018) 633–642.
- [9] F. Heidenau, W. Mittelmeier, R. Detsch, M. Haenle, F. Stenzel, G. Ziegler, H. Gollwitzer, A novel antibacterial titania coating: metal ion toxicity and in vitro surface colonization, J. Mater. Sci. Mater. Med. 16 (2005) 883–888.
- [10] V. Stranak, H. Wulff, H. Rebl, C. Zietz, K. Arndt, R. Bogdanowicz, B. Nebe, R. Bader, A. Podbielski, Z. Hubicka, R. Hippler, Deposition of thin titanium—copper films with antimicrobial effect by advanced magnetron sputtering methods, Mater. Sci. Eng. C 31 (2011) 1512—1519.
- [11] E. Zhang, F. Li, H. Wang, J. Liu, C. Wang, M. Li, K. Yang, A new antibacterial titanium-copper sintered alloy: preparation and antibacterial property, Mater. Sci. Eng. C 33 (2013) 4280–4287.
- [12] J. Liu, F. Li, C. Liu, H. Wang, B. Ren, K. Yang, E. Zhang, Effect of Cu content on the antibacterial activity of titanium-copper sintered alloys, Mater. Sci. Eng. C 35 (2014) 392–400.
- [13] E. Zhang, X. Wang, M. Chen, B. Hou, Effect of the existing form of Cu element on the mechanical properties, bio-corrosion and antibacterial properties of Ti-Cu alloys for biomedical application, Mater. Sci. Eng. C 69 (2016) 1210–1221.
- [14] I.F. Scheiber, J.L. Mercer, R. Dringen, Metabolism and functions of copper in brain, Prog. Neurobiol. 116 (2014) 33–57.
- [15] M. Niinomi, M. Nakai, Titanium-based biomaterials for preventing stress shielding between implant devices and bone, Int. J. Biomater. 2011 (2011), 836587.
- [16] L.E. Murr, Strategies for creating living, additively manufactured, opencellular metal and alloy implants by promoting osseointegration, osteoinduction and vascularization: an overview, J. Mater. Sci. Technol. 35 (2019) 231–241
- [17] B.V. Krishna, S. Bose, A. Bandyopadhyay, Low stiffness porous Ti strictures for load bearing implants, Acta Biomater. 3 (2007) 997–1006.
- [18] M. Mour, D. Das, T. Winkler, E. Hoenig, G. Mielke, M.M. Morlock, A.F. Schilling, Advances in porous biomaterials for dental and orthopaedic applications, Materials 3 (2010) 2947–2974.
- [19] G. Ryan, A. Pandit, D.P. Apatsidis, Fabrication methods of porous metals for use in orthopaedic application, Biomaterials 27 (2006) 2651–2670.
- [20] E. Zhang, J. Ren, S. Li, L. Yang, G. Qin, Optimization of mechanical properties, biocorrosion properties and antibacterial properties of as-cast Ti-Cu alloys, Biomed. Mater. 11 (2016), 065001.
- [21] Y.H. Li, N. Chen, H.T. Cui, F. Wang, Fabrication and characterization of porous Ti-10Cu alloy for biomedical application, J. Alloy. Comp. 723 (2017) 967–973.
- [22] C. Liu, Y. Liu, Y. Yang, Y. Ma, W. Liu, S. Tang, B. Liu, Q. Cai, New method for preparing micron porous aluminum via powder metallurgy, Mater. Sci. Technol. 34 (2018) 1295—1302.
- [23] A. Maznoy, A. Kirdyashkin, V. kitler, N. Pichugin, V. Salamatov, K. Tcoi, Self-propagating high-temperature synthesis of macroporous B2+L1<sub>2</sub> Ni-Al intermetallics used in cylindrical radiant burners, J. Alloy. Comp. 792 (2019) 561–573.
- [24] K. Essa, P. Jamshidi, J. Zou, M.M. Attallah, H. Hassanin, Porosity control in 316L stainless steel using cold and hot isostatic pressing, Mater. Des. 138 (2018) 21–29.
- [25] L. Zhang, Y.Q. Zhang, Y.H. Jiang, R. Zhou, Superelastic behaviors of biomedical porous NiTi alloy with high porosity and large pore size prepared by spark plasma sintering, J. Alloy. Comp. 644 (2015) 513–522.
- [26] E.K. Papynov, A.S. Portnyagin, E.B. Modin, V.Y. Mayorov, O.O. Shichalin, A.P. Golikov, V.S. Pechnikov, E.A. Gridasova, I.G. Tananaev, V.A. Avramenko, A complex approach to assessing porous structure of structured ceramics obtained by SPS technique, Mater. Char. 145 (2018) 294–302.
- [27] Z. Wang, C. Wang, C. Li, Y. Qin, L. Zhong, B. Chen, Z. Li, H. Liu, F. Chang, J. Wang, Analysis of factors influencing bone ingrowth into three-dimensional printed porous metal scaffolds: a review, J. Alloy. Comp. 717 (2017) 271–285.

- [28] P. Sharma, P.M. Pandey, Morphological and mechanical characterization of topologically ordered open cell porous iron foam fabricated using 3D printing and pressureless microwave sintering, Mater. Des. 160 (2018) 442–454.
- [29] J.L. Xu, S.C. Tao, L.Z. Bao, J.M. Luo, Y.F. Zheng, Effects of Mo contents on the microstructure, properties and cytocompatibility of the microwave sintered porous Ti-Mo alloys, Mater. Sci. Eng. C 97 (2019) 156–165.
- [30] M.K. Ibrahim, E. Hamzah, S.N. Saud, E.M. Nazim, A. Bahador, Parameter optimization of microwave sintering porous Ti-23%Nb shape memory alloys for biomedical applications, Trans. Nonferrous Metals Soc. China 28 (2018) 700-710.
- [31] M. Oghbaei, O. Mirzaee, Microwave versus conventional sintering: a review of fundamentals, advantages and applications, J. Alloy. Comp. 494 (2010) 175–189.
- [32] D.E. Khaled, N. Novas, J.A. Gazquez, F.M. Agugliaro, Microwave dielectric heating: applications on metals processing, Renew. Sustain. Energy Rev. 82 (2018) 2880–2892.
- [33] QB/T 2591, Antimicrobial Plastics—Test for Antimicrobial Activity and Efficacy, 2003.
- [34] J.L. Xu, L.Z. Bao, A.H. Liu, X.F. Jin, J.M. Luo, Z.C. Zhong, Y.F. Zheng, Effect of pore sizes on the microstructure and properties of the biomedical porous NiTi alloys prepared by microwave sintering, J. Alloy. Comp. 645 (2015) 137–142.
- [35] B.Y. Li, L.J. Rong, Y.Y. Li, The influence of addition of TiH<sub>2</sub> in elemental powder sintering porous Ni-Ti alloys, Mater. Sci. Eng. A 281 (2000) 169–175.
- [36] X. Yao, Q.Y. Sun, L. Xiao, J. Sun, Effect of Ti<sub>2</sub>Cu precipitates on mechanical behavior of Ti–2.5Cu alloy subjected to different heat treatments, J. Alloy. Comp. 484 (2009) 196–202.
- [37] L.L. Hench, Bioceramics, J. Am. Ceram. Soc. 81 (1998) 1705–1728.
- [38] Y.L. Zhou, D.M. Luo, Microstructures and mechanical properties of Ti-Mo alloys cold-rolled and heat heated, Mater. Char. 62 (2011) 931–937.
  [39] Y. Liu, S. Li, W. Hou, S. Wang, Y. Hao, R. Yang, T.B. Sercombe, L.C. Zhang,
- [39] Y. Liu, S. Li, W. Hou, S. Wang, Y. Hao, R. Yang, T.B. Sercombe, L.C. Zhang, Electron beam melted beta-type Ti-24Nb-4Zr-8Sn porous structures with high strength-to-modulus ratio, J. Mater. Sci. Technol. 32 (2016) 505–508.
- [40] H. Attar, L. Löber, A. Funk, M. Calin, L.C. Zhang, K.G. Prashanth, S. Scudino, Y.S. Zhang, J. Eckert, Mechanical behavior of porous commercially pure Ti and Ti-TiB composite materials manufactured by selective laser melting, Mater. Sci. Eng. A 625 (2015) 350–365.

- [41] G.İ. Nakaş, A.F. Dericioglu, Ş. Bor, Fatigue behavior of TiNi foams processed by the magnesium space holder technique, J. Mech. Behav. Biomed. 4 (2011) 2017–2023.
- [42] M. Niinomi, Mechanical properties of biomedical titanium alloys, Mater. Sci. Eng. A 243 (1998) 231–236.
- [43] X. Zhang, G.Y. Xiao, C.C. Jiang, B. Liu, N.B. Li, R.F. Zhu, Y.P. Lu, Influence of process parameters on microstructure and corrosion properties of hopeite coating on stainless steel, Corros. Sci. 94 (2015) 428–437.
- [44] C. Andrade, C. Alonso, Test methods for on-site corrosion rate measurement of steel reinforcement in concrete by means of the polarization resistance method, Mater. Struct. 37 (2004) 623–643.
- [45] J.L. Xu, X.F. Jin, J.M. Luo, Z.C. Zhong, Fabrication and properties of porous NiTi alloys by microwave sintering for biomedical application, Mater. Lett. 124 (2014) 110–112.
- [46] X.T. Sun, Z.X. Kang, X.L. Zhang, H.J. Jiang, R.F. Guan, X.P. Zhang, A comparative study on the corrosion behavior of porous and dense NiTi shape memory alloys in NaCl solution, Electrochim. Acta 56 (2011) 6389–6396.
- [47] R. Liu, Y. Tang, L. Zeng, Y. Zhao, Z. Ma, Z. Sun, L. Xiang, L. Ren, K. Yang, In vitro and in vivo studies of anti-bacterial copper-bearing titanium alloy for dental application, Dent. Mater. 34 (2018) 1112–1126.
- [48] M. Bao, Y. Liu, X. Wang, L. Yang, S. Li, J. Ren, G. Qin, E. Zhang, Optimization of mechanical properties, biocorrosion properties and antibacterial properties of wrought Ti-3Cu alloy by heat treatment, Bioact. Mater. 3 (2018) 28–38.
- [49] J. Liu, X. Zhang, H. Wang, F. Li, M. Li, K. Yang, E. Zhang, The antibacterial properties and biocompatibility of a Ti-Cu sintered alloy for biomedical application. Biomed. Mater. 9 (2014), 025013.
- [50] L. Fowler, O. Janson, H. Engqvist, S. Norgren, C. Öhman-Mägi, Antibacterial investigation of titanium-copper alloys using luminescent Staphylococcus epidermidis in a direct contact test, Mater. Sci. Eng. C 97 (2019) 707–714.
- [51] Q.L. Feng, T.N. Kim, J. Wu, E.S. Park, J.O. Kim, D.Y. Lim, F.Z. Cui, Antibacterial effects of Ag-HAp thin films on alumina substrates, Thin Solid Films 335 (1998) 214–219.
- [52] L.B. Boinovich, E.B. Modin, A.V. Aleshkin, K.A. Emelyanenko, E.R. Zulkarneev, I.A. Kiseleva, A.L. Vasiliev, A.M. Emelyanenko, Effective antibacterial nanotextured surfaces based on extreme wettability and bacteriophage seeding, ACS Appl. Nano Mater. 1 (2018) 1348–1359.